JVSTB Journal of Vacuum Science & Technology B

Secondary ion and neutral mass spectrometry with swift heavy ions: Organic molecules

Lars Breuer, Florian Meinerzhagen, Matthias Herder, Markus Bender, Daniel Severin, Jordan O. Lerach, and Andreas Wucher

Citation: Journal of Vacuum Science & Technology B **34**, 03H130 (2016); doi: 10.1116/1.4943158
View online: http://dx.doi.org/10.1116/1.4943158
View Table of Contents: http://scitation.aip.org/content/avs/journal/jvstb/34/3?ver=pdfcov
Published by the AVS: Science & Technology of Materials, Interfaces, and Processing

Secondary ion and neutral mass spectrometry with swift heavy ions: Organic molecules

Lars Breuer, Florian Meinerzhagen, and Matthias Herder
Fakultät für Physik, Universität Duisburg-Essen, Lotharstr. 1-21, D-47048 Duisburg, Germany

Markus Bender and Daniel Severin
Gesellschaft für Schwerionenforschung GSI, Planckstr. 1, D-64291 Darmstadt, Germany

Jordan O. Lerach
Department of Chemistry, Eberly College of Science, The Pennsylvania State University, 213 Chemistry Building, University Park, Pennsylvania 16802

Andreas Wucher[a)]
Fakultät für Physik, Universität Duisburg-Essen, Lotharstr. 1-21, D-47048 Duisburg, Germany

(Received 15 November 2015; accepted 22 February 2016; published 24 March 2016)

The authors report on experiments regarding the electronic and nuclear sputtering of organic films. The newly built swift heavy ion induced particle emission and surface modifications setup [Meinerzhagen *et al.*, Rev. Sci. Instrum. **87**, 013903 (2016)] at the M1 Branch at the universal linear accelerator (UNILAC) beam line at GSI in Darmstadt, Germany, has been used for research on organic molecules in the electronic sputtering regime. This setup has the unique capability not only to investigate electronically sputtered ions by projectiles with kinetic energies up to several giga-electron-volt but also to detect their neutral counterparts as well by laser postionization. For this purpose, the experiment is equipped with a laser system delivering 157 nm pulses with photon energies of 7.9 eV to be utilized in single photon ionization. In addition to the investigation of sputtered ions and neutrals in the electronic sputtering regime, a comparison of typical fragments between fundamentally different sputtering mechanisms has been performed by using two different common time of flight secondary ion mass spectrometry (SIMS) instruments. The use of the different instruments offers the possibility to investigate the influence of the differing sputter processes from the linear cascade regime over collisional spikes to the thermal spike regime under high energy ion bombardment. The experiments in the collision-dominated nuclear stopping regime have been performed using 20 keV Bi^+ and Bi_3^+ as atomic and small cluster projectiles and using 20 keV C_{60}^+ representing a medium-sized cluster. In the electronic sputtering regime, 4.8 MeV/u $^{197}Au^{26+}$ swift heavy ions created by the UNILAC have been used as projectiles. As targets thin films of coronene on silicon substrates, a polycyclic hydrocarbon and Irganox 1010, an antioxidant well known from different studies in the SIMS community, have been utilized. © *2016 American Vacuum Society*. [http://dx.doi.org/10.1116/1.4943158]

I. INTRODUCTION

One of the main goals in the analysis of organic samples with time-of-flight secondary ion mass spectrometry (ToF-SIMS) is to detect intact molecular ions without significant fragmentation. Due to the violent nature of a linear collision cascade, this goal cannot be achieved in general with common ion sources, which deliver atomic ion beams with kinetic energies of several kilo-electron-volts. A recent development in the field is the use of cluster ion sources, which provide ion beams of small metal, C_{60} (Ref. 1) or even large noble gas cluster such as Ar_n with n up to 10 000.[2–4] The invention of these types of ion sources makes it possible to conserve molecular information even during depth profiling through organic samples due to a shift in the emission process from the linear-cascade to a spike-dominated regime where a phase explosion or collisional spike takes place. In this regime, the collision induced fragmentation and the build-up of damage in subsurface layers is reduced by an energy deposition closer to the surface. Another possible way to shift the emission process away from the linear cascade into the spike regime is the use of swift heavy ions (SHI) with total energies up to some giga-electron-volt.

The first experiments in the electronic sputtering regime have been made with Californium ion sources, using high energetic fission fragments statistically produced by radioactive decay as primary particles. This technique, called plasma desorption mass spectrometry,[5] provides the possibility of fundamentally changing the energy transfer from the projectile into the solid. In the regime of primary particles with kinetic energies of several kilo-electron-volts, the energy transfer is dominated by collisions between the projectile and target atoms. These processes dramatically change upon increasing the energy into the regime of several mega-electron-volts per nucleon. In this case, nuclear stopping becomes almost negligible and the direct energy transfer from the projectile to the electronic subsystem of the solid (electronic stopping) becomes the dominant energy

a)Electronic mail: andreas.wucher@uni-due.de

dissipation process. The electronic stopping cross section reaches a maximum at an impact energy around several mega-electron-volts per nucleon, which for gold projectiles corresponds to approximately 1 GeV total kinetic energy. The energy transferred to the electrons is spatially spread away from the ion track and transferred to the nuclear subsystem via electron–phonon coupling, which—among other effects—may lead to particle emission into the vacuum. This "electronic sputtering" processes can be described by the inelastic thermal-spike model,[6–8] which predicts a localized rapid critical overheating of the material followed by either thermal evaporation or a fluid dynamical phase explosion, leading to particle emission.

The universal linear accelerator (UNILAC) at GSI in Darmstadt, Germany, provides the capability to generate ions of all stable isotopes from hydrogen to uranium and accelerate them to kinetic energies between 3.6 and 11.4 MeV/u. Moreover, it is possible to select the charge state of the accelerated ions, providing the possibility to investigate the influence of the kinetic energy, charge state, and mass of the primary particle on the emission and ionization process of electronically sputtered material. We have recently coupled this ion beam with a ToF mass spectrometer by integrating a ToF-SIMS/secondary neutral mass spectrometry (SNMS) instrument into the beam line at the UNILAC.[9] As a unique feature, this setup allows to detect both the *ionic* and *neutral* components of the sputtered material, thereby allowing a comprehensive characterization of the sputtered flux. In this study, we report our initial experiments performed with this setup on organic films irradiated by 4.8 MeV/u gold ions. ToF-SIMS studies on molecular ion emission under SHI bombardment have been reported before,[10–15] indicating that electronic sputtering might be a possible strategy to "softly" desorb intact molecules with minimal amount of fragmentation. These experiments, however, have been conducted at lower kinetic energies where electronic and nuclear stopping are of comparable magnitude and, most importantly, were restricted to the ionic component of the sputtered material. In contrast, the kinetic energy employed here corresponds to the maximum of the electronic stopping cross section where nuclear stopping is practically negligible, thereby allowing to investigate the purely electronic sputtering process with a particular emphasis on (1) the comparison of secondary ion and neutral molecule emission, and (2) the molecular fragmentation associated with the emission process. In order to compare particularly the latter with the collision-dominated nuclear sputtering process, this study also includes comparative experiments performed with common kilo-electron-volt ToF-SIMS instruments equipped with a variety of different ion sources, including atomic and cluster projectile beams.

As organic model systems, Coronene and Irganox 1010 have been used in this study. Coronene ($C_{24}H_{12}$, molecular weight 300 g/mol) is an ideal model molecule due to its simple structure, low ionization potential [7.2 eV (Ref. 16)], and stability with respect to ionization due to its aromaticity. The more complex and fragile molecule Irganox 1010 ($C_{73}H_{108}O_{12}$, molecular weight 1178 g/mol) has been well investigated by several studies in the SIMS community. With respect to the single photon postionization method employed here, it represents a contrast to the coronene molecule since its ionization potential is above the photon energy of 7.9 eV.

II. EXPERIMENT

The experiments using SHI as primary particles have been performed at the swift heavy ion induced particle emission and surface modifications experimental setup at the M1-Branch of the UNILAC beam line at GSI, which has been described in great detail elsewhere.[9] Briefly, the system consists of several ultra high vacuum (UHV)-chambers for sample preparation and storage, which are not exposed to the SHI beam, and an irradiation chamber at the end of the M1-Branch of the UNILAC beam-line. Figure 1 shows a sketch of the experimental setup in the irradiation chamber. A home built time-of-flight reflectron type mass-spectrometer[17,18] is mounted to the irradiation chamber at an angle of 45° with respect to the incoming SHI beam. A commercially available 5 keV hot cathode type rare gas ion source (Leybold, IQ-100) is mounted to the chamber and used for spectrometer and sample alignment (see below). The sample is positioned using a computer controlled stage and aligned such that the surface normal and the SHI beam are creating an angle of 45°, and the surface normal is parallel to the ion optical axis of the spectrometer. During the ion bombardment of the sample, the extraction field is pulsed off to ensure a field free expansion of the sputtered ions and neutrals. The plume of sputtered particles is intersected by a pulsed vacuum ultraviolet laser-beam of a wavelength of 157 nm. This wavelength corresponds to a photon energy of $E_{Ph} = 7.9$ eV, thereby allowing single-photon ionization of sputtered neutrals with ionization potentials up to this value.

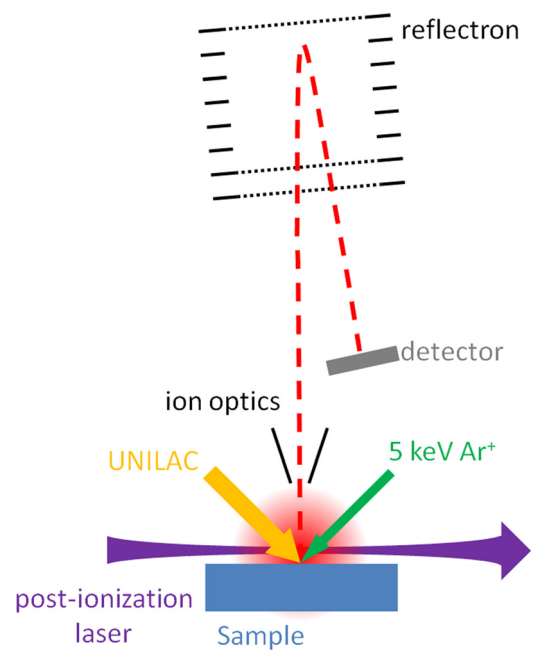

FIG. 1. (Color online) Experimental setup at the M1-branch of the UNILAC beam line.

The secondary ions and postionized secondary neutrals are extracted into the spectrometer via an electric field created by switching the sample potential to high voltage at a delay of about 10 ns after the ionization laser was fired. This method ensures the same experimental conditions with respect to instrument transmission, detection probability, probed emission velocity interval, etc., for extracted secondary ions and postionized neutrals. The ions are detected by a Chevron stack of two microchannel plates (MCP). In order to boost the detection probability of molecules, the detector was operated at a post-acceleration voltage of 4 kV applied to the MCP front.

For the purpose of adjusting the ion optical parameters of the spectrometer, the 5-keV Ar^+ beam was used, which points at the analyzed surface under approximately the same polar angle as the SHI beam. For alignment purposes, an elemental (metal) target was used, and the position of the kilo-electron-volt beam was optimized to maximize the detected secondary ion signal. Then, the SHI beam was overlapped with the kilo-electron-volt ion beam using the light emitted from the irradiated spot on a chromium doped Al_2O_3 target. More specifically, the position of the keV beam is marked within a camera image of the sample surface, and afterwards, the SHI beam is collimated by an adjustable aperture and focused onto the marked spot using quadrupole magnet pairs. In any case, it is made sure that both ion beams irradiate a spot, which is much larger than the surface area probed by the ToF spectrometer. An observation, which has been made during several experiments on different materials, is that during SHI irradiation, the sample often starts to emit photons as well, which are observable on the camera screen. As a general trend, we find that a strong light emission is coupled with strong mass spectrometric signals as well, indicating a relatively high total sputter yield.

The UNILAC delivers ion pulses of 1–5 ms duration at 1–50 Hz repetition rate with average ion currents between 0.1 and 10 nA. For the experiments using SHI as projectiles reported here, the pulse duration was 3 ms at 10 Hz repetition rate with an average ion current of 0.3 nA. In connection with the ion charge state (+26) and the irradiated spot ($\sim$0.4 cm^2), this corresponds to an ion fluence of about 2×10^7 cm^2 per pulse. Due to the long primary ion pulse duration, a timing scheme adapted to the temporal structure of the UNILAC beam pulses was applied. As described in detail elsewhere,[1,19] the relatively long SHI pulses were treated as a quasi-dc ion beam, and the temporal resolution of the ToF measurement was provided by fast switching of the ion extraction field as in delayed extraction mode. This way, ions (i.e., secondary ions or postionized neutrals) which are present in the sensitive volume at the time when the extraction field is switched on are swept into the ToF spectrometer, time focused in the reflectron, and detected in a sharp flight time peak with a mass resolution of about $m/\Delta m \sim 300$. Secondary ions leaving the surface while the extraction field is switched on are suppressed by setting the reflector potential slightly below the sample potential. Spectrum acquisition was performed at the highest sustainable repetition rate (up to 10 kHz), so that bursts of multiple spectra could be acquired during a single accelerator pulse of several milliseconds duration. Since the postionization laser can only sustain a maximum repetition rate of 500 Hz, it was only fired during the first of these spectra, making this one an SNMS spectrum and leaving the remaining spectra in each burst to contribute to the corresponding SIMS spectrum. In addition, control spectra with either the kilo-electron-volt ion beam or with no ion bombardment at all were taken with the same burst strategy during the relatively long pause between subsequent SHI pulses, again interleaved as SNMS/SIMS, thereby making the most efficient use of valuable beam time.

Postionization of sputtered neutral particles is accomplished by means of a pulsed F_2 excimer laser (ATLEX 500 -L, ATL Lasertechnik GmbH) delivering pulses with energies up to 1.7 mJ at a wavelength of 157 nm and a FWHM duration of 5–8 ns. The laser beam is coupled to the UHV chamber via an evacuated beam line including an adjustable dielectrical mirror designed for 157 nm radiation and a movable CaF_2 lens with a focal length of 209 mm. The lens is mounted on an UHV xy-manipulator, and the beam is steered by moving the lens in order to intersect the plume of sputtered particles in a direction approximately parallel to and at a height of about 1 mm above the sample surface. The exact position of the laser focus is adjusted such as to optimally overlap the laser beam with the sensitive volume of the ToF spectrometer.

The experiments with C_{60} primary beams were performed at our lab in Duisburg using a different reflectron type mass spectrometer described elsewhere.[20] In this case, the typical ToF-SIMS/SNMS timing scheme was used with a pulsed primary ion beam (pulse duration several microseconds) and delayed extraction. In addition, ToF-SIMS spectra of coronene were collected using Bi^+ and Bi_3^+ primary ions on a commercial ToF-SIMS instrument (TOF_SIMS V, IonTof GmbH).

The coronene samples used in this study have been prepared using physical vapor deposition as described in detail elsewhere.[21] The Irganox 1010 sample was provided by the National Physical Laboratory in England.

III. RESULTS AND DISCUSSION

As outlined in the Introduction, the goal of this work was to investigate the emission of molecular species—ions and neutrals—which are sputtered under SHI bombardment from organic layers. Irganox 1010 and coronene films were used as target materials, which were bombarded with 4.8 MeV/u $^{197}Au^{26+}$ projectiles (a total kinetic energy of 0.95 GeV).

A. Irganox 1010

Irganox 1010 has been investigated many times with common ToF-SIMS systems. The recorded mass spectra typically show a strong $[M\text{-}H]^-$ signal in the negative ion spectrum, while the $[M+H]^+$ in the positive ion spectrum is weak in comparison. Due to the high kinetic energy of the projectiles, the energy transfer to the organic film is dominated by electronic stopping of the projectile. The projectile passes through the thin film (thickness of a couple of

hundreds of nanometers) and comes to a full stop in the silicon substrate.

Figure 2(b) shows the negative ion spectrum with identified peaks. The two dominant peaks in this spectrum are the typical fragment at m/z 213 ($C_{16}H_{23}O$) and the molecular ion ($[M\text{-}H]^-$) at m/z 1176. It is interesting to compare this spectrum with spectra obtained under kilo-electron-volt cluster bombardment, where the emission process is governed by a collisional spike. Unlike the spectra typically obtained under C_{60}^+ bombardment,[22] the spectrum in Fig. 2(b) is not dominated by low mass fragments below a mass of 100 amu. Another striking observation is that some typical fragments in the mass range around 800 and 900 amu show different patterns compared to C_{60}^+ bombardment, which may indicate different fragmentation channels due to the different energy dissipation channel of the primary particle.

A close look at the positive spectrum presented in Fig. 2(a) reveals a weak $[M+H]^+$ signal, as expected from experiments with keV cluster ion sources, such as C_{60}^+. Nevertheless, it is interesting to note that the protonated molecule can be observed under these high energy bombardment conditions, followed by a group associated with fragments which are all equally spaced by 57 amu, representing the terminating tert-butyl groups of the benzene rings at each arm of the molecule. These fragments can be found as a strong peak at m/z 57 in the low mass region of the spectrum. The dominant peak in this spectrum appears at m/z 233, which represents a characteristic fragment ($C_{16}H_{25}O$) of one the four arms of the molecule. A comparison of the SIMS and SNMS spectra reveals that there is no gain in the molecular ion signal by the use of the postionization laser. While the photon energy of the postionization laser (7.9 eV) is obviously not sufficient to overcome the ionization potential of Irganox 1010, an increase in the signal of the characteristic fragments of this molecule can be observed. This increase is outstanding for the tert-*butyl* groups at m/z 57 and the characteristic fragment at m/z 213.

Another interesting feature is the temporal behavior of the measured signals during a single accelerator ion pulse cycle. This was followed by changing the timing scheme of the experiment such that SNMS and SIMS spectra were taken at different times with respect to the start of the SHI ion pulse. As a result, we find that additional signals at m/z 243, 245 and 247 amu appear in the SNMS spectra when the data are taken at later times during the SHI pulse. The temporal behavior of these signals is shown in Fig. 3. An exponential increase is observed at the beginning of the primary ion pulse, with the signals reaching a maximum at approximately 1.3 ms after the start of the bombardment. After the end of the ion bombardment, the signal stays and shows an exponential decay. In contrast to that observation, the secondary ion signal exhibits a temporal behavior that mirrors the shape of the accelerator pulse, i.e., the variation of the projectile ion current during the pulse. These observations suggest that the peak group around m/z 245 is induced by a thermal evaporation process due to the ion bombardment induced macroscopic heating of the material during one single accelerator pulse.

Following that finding, the signals of secondary ions (SIMS) and their postionized neutral counterparts (SNMS) at m/z 57 and 219 representing characteristic fragments of

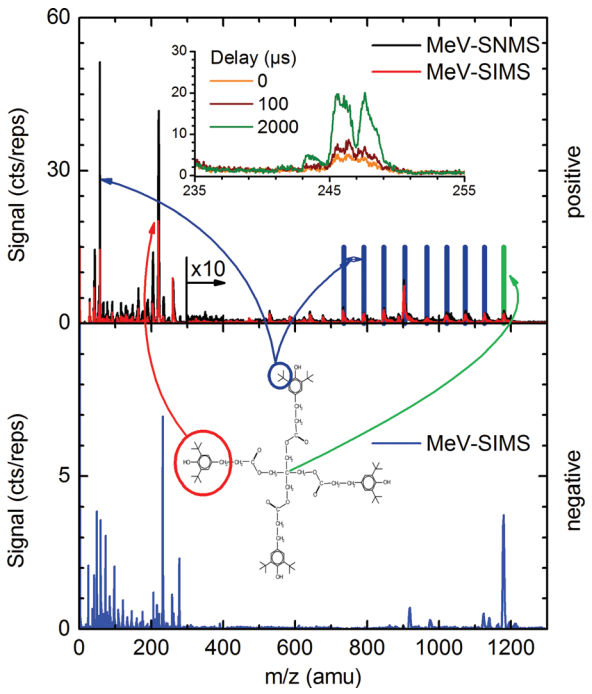

FIG. 2. (Color) (a) Positive ion spectrum of Irganox 1010 under 4.8 MeV/u $^{197}Au^{26+}$ bombardment. The red line represents the SIMS spectrum containing only the secondary ion signal. The black line represents the SNMS spectrum containing the secondary ions and postionized neutrals. Starting at m/z = 300 the signal axis has been spread ten times. The inlet shows the peak group around mass 245 at different times during the ion bombardment. Time zero corresponds to the beginning of the UNILAC pulse. (b) Negative secondary ion spectrum of Irganox 1010.

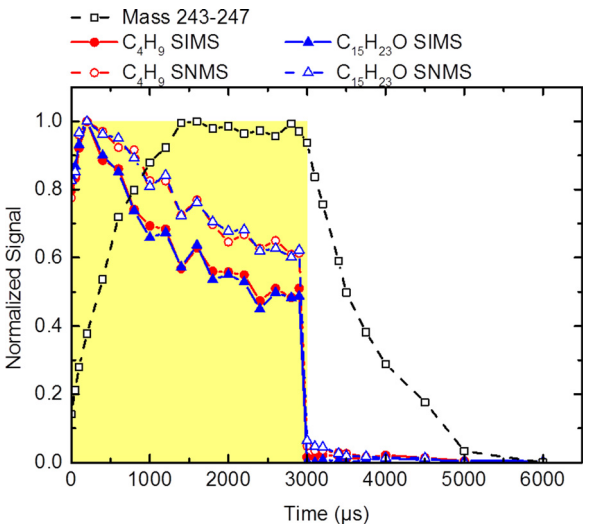

FIG. 3. (Color online) Time dependence of typical fragment signals of the Irganox 1010 molecule at m/z 57 and 219 during a single SHI primary ion pulse. The solid lines and data points represent the SIMS signals, and the dashed lines and open data points represent the SNMS signals. The shaded area indicates the temporal duration of the accelerator pulse. The dashed line with open squared data points represents an unidentified peak group around m/z 245 only appearing in the postionized neutral spectrum.

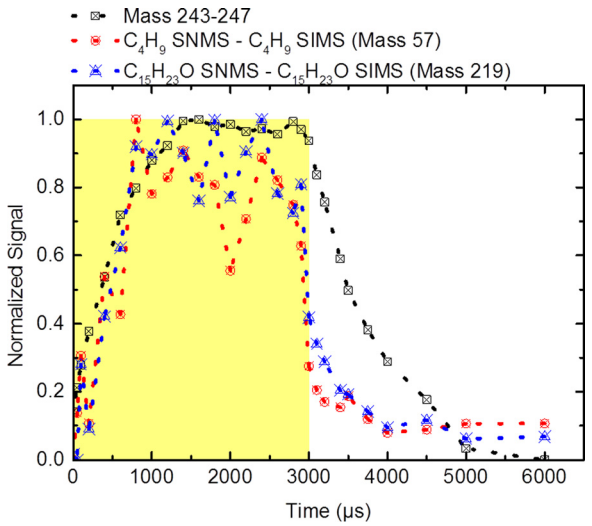

FIG. 4. (Color online) Difference between the SNMS and SIMS signals of Irganox1010 fragments at m/z 57 and 219 displayed in Fig. 3 normalized to their respective maximum values.

Irganox1010 have been normalized to the respective signal maximum and plotted as a function of time in Fig. 3. The SIMS and SNMS signals are reaching their maximum approximately 200 μs after the start of the bombardment, reflecting the rise time of primary ion pulse. With the ongoing bombardment, however, a significant difference between the SIMS and the SNMS signals can be observed. More specifically, a gap between both signals is opening and an SNMS signal can still be observed after the end of the SHI pulse. These findings indicate that two different emission processes take place particularly for the detected neutral particles. On one hand, sputtered particles are formed whose temporal emission behavior strictly follows the temporal profile of the primary ion current. On the other hand, thermally evaporated particles, due to fast heating of the sample during the primary ion pulse, are emitted from the surface. The fact that emitted particles can be detected after the end of the primary ion pulse strongly supports this interpretation. By subtracting the normalized SIMS from the normalized SNMS signal, the relative contribution of thermally emitted particles to the neutral spectrum can be extracted in more detail. The result is shown in Fig. 4 and closely resembles that found for the peak group around m/z 245.

B. Coronene

Previous studies of Willingham *et al.* using IR strong-field ionization as postionization mechanism and 20 keV Au^+ and 20 keV C_{60}^+ primary ion beams already showed the influence of the softer sputtering mechanism using cluster projectiles.[21] In our study, three different instruments and four different primary ion beams have been used.

The spectra obtained for a coronene film irradiated with 4.8 MeV/u $^{197}Au^{26+}$ ions are shown in Fig. 5. Probeably the most important observation is the very large signal of intact postionized neutral molecules which completely dominates the spectrum to such an extent that the detector gain had to be reduced in order to avoid saturation of the molecular ion peak (blue line in the lower panel of Fig. 5). With this detector setting, all remaining peaks in the spectrum fall close to the noise limit, so that the spectrum was recorded again using the full detector gain and scaled by matching the intensity of the $[M-2C]^+$ fragment ion peak at m/z 276 (red line in Fig. 5).

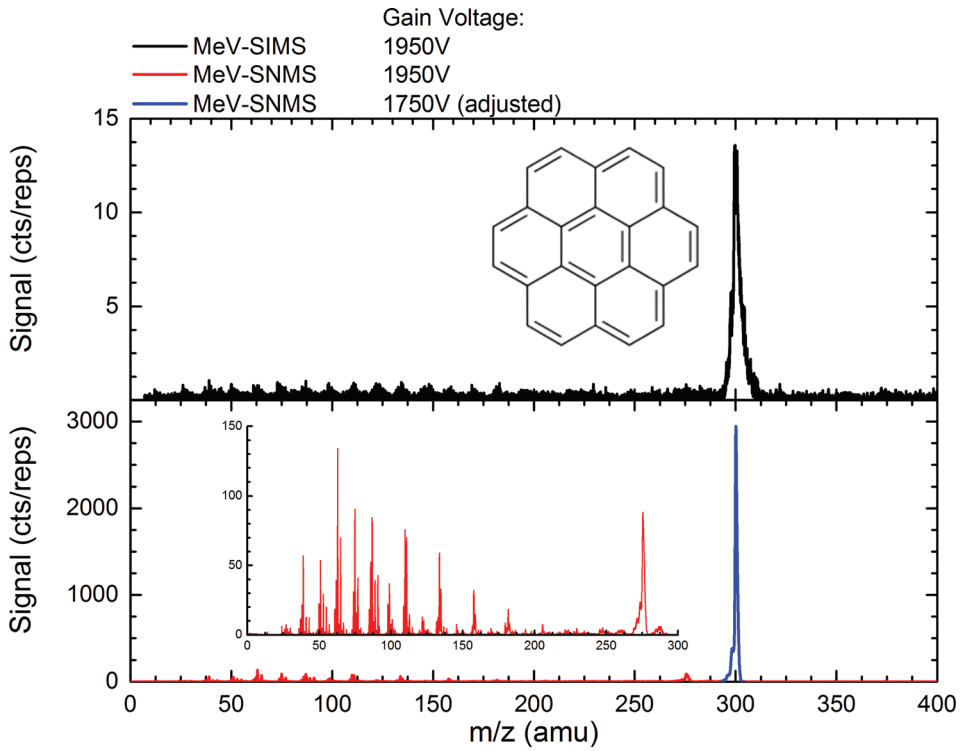

FIG. 5. (Color) Positive ion spectra of coronene bombarded by 4.8 MeV/u $^{197}Au^{26+}$ ions. Upper panel: SIMS spectrum taken at full detector gain. Lower panel: SNMS spectrum scaled regarding to different detector gain voltages applied for the molecular ion and the rest of the spectrum.

It is evident that all other peaks in the recorded SNMS spectrum exhibit at least 2 orders of magnitude less intensity than the molecular ion peak, indicating nearly fragment-free desorption of intact neutral molecules under SHI bombardment. As seen in the upper panel of Fig. 5, the SIMS spectrum is also dominated by the molecular ion peak, albeit at much lower intensity. Comparing the peak maximum in both spectra, we find a SIMS/SNMS ratio of 4×10^{-3} characterizing the ion fraction of a sputtered coronene molecule during the emission process. Note that this value represents an upper limit to the true ionization probability, since the detected SNMS signal may still underestimate the neutral yield due to incomplete postionization.

Another important observation is that the blank SNMS spectrum taken without ion bombardment also shows a weak molecular ion signal. This spectrum represents a residual gas spectrum, where gas phase species present in the ionization volume are photoionized by the postionization laser. Note that this spectrum was taken at a delay of about 15 ms after the end of the SHI pulse. The observed molecular ion signal must therefore be generated due to thermal evaporation of intact coronene molecules from the molecular layer in the UHV. To ensure that this effect does not have the same origin as the additional peaks for the Irganox 1010, a similar pulse map as depicted in Fig. 3 was collected with and without postionization. The resulting temporal behavior of the coronene SIMS and SNMS signal is depicted in Fig. 6. Besides pulse shape fluctuations between subsequent UNILAC pulses,[19] no statistically significant difference between both desorption processes can be found. Even though the coronene molecule is evaporating without ion irradiation, we therefore find no indication of a thermal desorption process due to ion irradiation induced heating as observed for the Irganox 1010 molecule.

Figure 7 shows the negative ion spectrum collected with the SHI beam. In this spectrum, the molecular ion cannot be observed, but a sequence of C_nH_m groups appears in the spectrum, which represent irradiation induced fragments of the coronene parent molecule. It is interesting to compare the relative intensity distribution among these groups

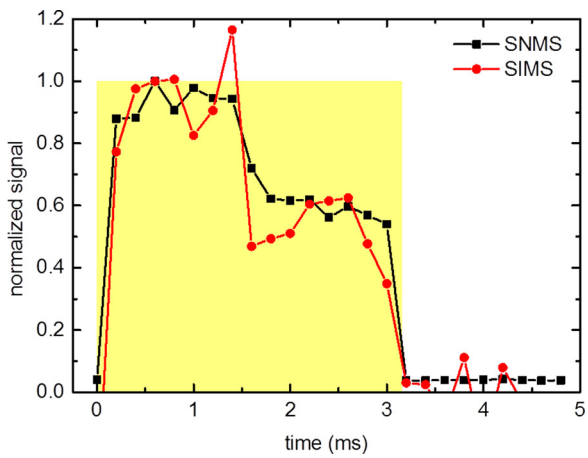

FIG. 6. (Color online) Time dependence of the molecular ion signal measured for coronene in the SIMS and SNMS mode. The shaded box indicates the temporal duration of the SHI primary ion pulse.

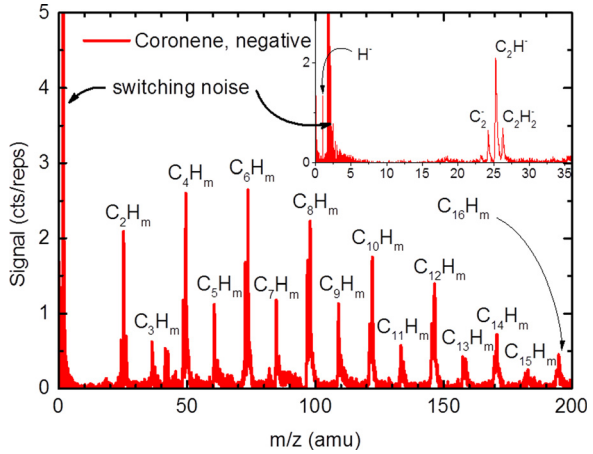

FIG. 7. (Color online) Negative ion spectrum of coronene fragments produced under $^{197}Au^{26+}$ bombardment. The peak around m/z 3 is noise arising from the switching of the stage potential.

between the mega-electron-volt per nucleon ion irradiation performed here and irradiation of similar samples produced by physical vapor deposition in the same batch with kilo-electron-volt atomic and cluster ion beams. As outlined in the experimental section, an IonTof TOFSIMS V instrument was used for experiments with atomic metal (30 keV Bi^+) and small cluster (30 keV Bi_3^+) projectiles, and the experiments with medium sized (20 keV C_{60}^+) cluster projectiles were performed on a Bio-ToF spectrometer. Figure 8 shows the resulting intensity distribution measured in these experiments. For better comparison, the peak integrals for the C_n,

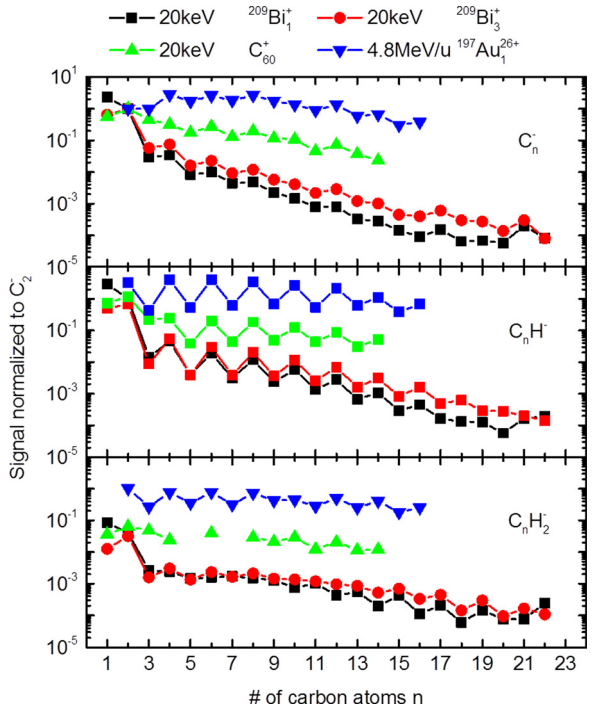

FIG. 8. (Color online) Signal intensity measured for different fragment ions produced under bombardment of coronene with different projectiles. The upper panel shows the signals for the different carbon clusters, the middle panel for the C_nH clusters and the lower panel for the C_nH_2 clusters. For each projectile, the signals have been normalized to the corresponding C_2 signal.

C_nH, and C_nH_2 groups have been normalized to the C_2 signals induced by the corresponding projectile. The C_2 peak was chosen because no sputtered atomic carbon was observed with the SHI beam. By comparing these intensity distributions, we observe that the majority of detected particles are from the low mass region and represent small fragments of coronene. It is clearly seen that the more the sputtering process is shifted from a linear collision cascade toward a spike emission of material, the more massive fragments can be detected. The linear-cascade regime, which is represented by sputtering with atomic Bi projectiles, shows the greatest amount of fragmentation, indicated by the steepest fall of the measured fragment intensity with the increasing fragment size. In this regime, the C signal is the dominant signal in the spectrum. The transition from the linear cascade regime to the collisional spike regime (Bi_3^+) already shows a larger contribution of larger fragments. This trend continues for the bombardment with C_{60}^+ projectiles, where the sputtering process can be described as a so-called phase explosion following rapid collisional heating of a shallow subsurface region. The electronic sputtering process, which is often described as a thermal spike, apparently shows the smallest amount of low mass fragments, while the medium sized fragments dominate the negative spectrum. These findings point at the conclusion that the electronic sputtering process indeed provides a suitable mechanism for "soft" desorption of molecules from an ion irradiated surface.

IV. SUMMARY AND CONCLUSIONS

The experiments presented in this work provide valuable information regarding the emission processes of molecules from organic layers under SHI bombardment. An important result is the increased probability to conserve the molecular ion information in sputtering with high energetic heavy ions, such as $^{197}Au^{26+}$ with a total kinetic energy of 0.95 GeV. This has been shown for a simple model molecule, coronene, for which intact neutral molecules are found to clearly dominate the composition of the sputtered material. Unfortunately, a similar statement cannot be made for the second molecule investigated here, Irganox 1010, due to the fact that the available photon energy is not large enough for single photon ionization of this molecule. Both molecules show the molecular secondary ion signals (or protonated molecules) in the ion spectrum measured under SHI bombardment. For coronene, it was found that the change of the sputtering from a linear cascade via the collisonal spike regime toward the "thermal" spike regime reduces the ratio of small mass fragments, indicating a less pronounced fragmentation of the molecules during the sputtering process. Both of these findings, the conservation of the molecular ion and the reduction of collision induced fragmentation, show that the use of SHI may be a valuable tool for soft desorption of molecules from solid surfaces without significant fragmentation.

With respect to SHI-SIMS applications, further investigations are planned in order to quantitatively determine the ionization probabilities of electronically sputtered molecules from the ratio of sputtered neutral to ion signals. These future experiments will contribute to the better understanding of the fundamental processes in sputtering and ionization during SHI bombardment.

ACKNOWLEDGMENTS

The authors would like to thank the German Ministry of Science (BMBF) for the financial support in the framework of the "Verbundpojekt 05K2013—Ion Induced Materials Characterization and Modification." The authors greatly thank A. Shard from the National Physical Laboratory (NPL), England, for providing the Irganox 1010 films.

[1]N. Winograd, Anal. Chem. **77**, 7 (2005).
[2]I. Yamada, J. Matsuo, N. Toyoda, and A. Kirkpatrick, Mater. Sci. Eng., R **34**, 231 (2001).
[3]I. Yamada, J. Matsuo, N. Toyoda, T. Aoki, E. Jones, and Z. Insepov, Mater. Sci. Eng., A **253**, 249 (1998).
[4]S. Ninomiya, Y. Nakata, K. Ichiki, T. Seki, T. Aoki, and J. Matsuo, Nucl. Instrum. Methods B **256**, 493 (2007).
[5]R. MacFarlane and D. Torgerson, Int. J. Mass Spectrom. **21**, 81 (1976).
[6]M. Toulemonde, E. Paumier, and C. Dufour, Radiat. Eff. Defect. Solids **126**, iii (1993).
[7]W. Assmann, M. Toulemonde, and C. Trautmann, *Sputtering by Particle Bombardment: Experiments and Computer Calculations from Threshold to MeV Energies*, edited by R. Behrisch and W. Eckstein (Springer-Verlag, Berlin/Heidelberg, 2007), pp. 401–451.
[8]M. Toulemonde, W. Assmann, C. Dufour, A. Meftah, and C. Trautmann, Nucl. Instrum. Methods B **277**, 28 (2012).
[9]F. Meinerzhagen, L. Breuer, H. Bukowska, M. Herder, M. Bender, D. Severin, H. Lebius, M. Schleberger, and A. Wucher, Rev. Sci. Instrum. **87,** 013903 (2016).
[10]B. N. Jones, J. Matsuo, Y. Nakata, H. Yamada, J. Watts, S. Hinder, V. Palitsin, and R. Webb, Surf. Interface Anal. **43**, 249 (2011).
[11]H. Yamada, K. Ichiki, Y. Nakata, S. Ninomiya, T. Seki, T. Aoki, and J. Matsuo, Nucl. Instrum. Methods B **268**, 1736 (2010).
[12]M. Fujii, M. Kusakari, K. Matsuda, N. Man, T. Seki, T. Aoki, and J. Matsuo, Surf. Interface Anal. **46**, 353 (2014).
[13]H. Hijazi *et al.*, Nucl. Instrum. Methods B **269**, 1003 (2011).
[14]H. Hijazi *et al.*, Eur. Phys. J. D **66**, 68 (2012).
[15]H. Hijazi *et al.*, Eur. Phys. J. D **66**, 305 (2012).
[16]D. Schröder, J. Loos, H. Schwarz, R. Thissen, D. V. Preda, L. T. Scott, D. Caraiman, M. V. Frach, and D. K. Böhme, Helv. Chim. Acta **84**, 1625 (2001).
[17]A. Wucher, M. Wahl, and H. Oechsner, Nucl. Instrum. Methods B **82**, 337 (1993).
[18]M. Wahl and A. Wucher, Nucl. Instrum. Methods B **94**, 36 (1994).
[19]L. Breuer, F. Meinerzhagen, M. Bender, D. Severin, and A. Wucher, Nucl. Instrum. Methods B **365**, 482 (2015).
[20]R. M. Braun, P. Blenkinsopp, S. J. Mullock, C. Corlett, K. F. Willey, J. C. Vickerman, and N. Winograd, Rapid Commun. Mass Spectrom. **12**, 1246 (1998).
[21]D. Willingham, A. Kucher, and N. Winograd, Appl. Surf. Sci. **255**, 831 (2008).
[22]The static SIMS library, V 4.0.1.35, Surface Spectra Ltd., Irganox 1010 with C_{60}^+ bombardment, Inst ID 26.